

Structure and Physical Properties of the Polar Oxysulfide CaZnOS

Timothy Sambrook, Catherine F. Smura, and Simon J. Clarke*

Inorganic Chemistry Laboratory, Department of Chemistry, University of Oxford, South Parks Road, Oxford OX1 3QR, U.K.

Kang Min Ok

Chemistry Research Laboratory, Department of Chemistry, University of Oxford, Mansfield Road, Oxford OX1 3TA, U.K.

P. Shiv Halasyamani

Department of Chemistry, University of Houston, 136 Fleming Building, Houston, Texas 77204-5003

Received November 7, 2006

The synthesis, structure, and electrical properties of the oxysulfide CaZnOS are reported. The white compound has a band gap of 3.7(1) eV and crystallizes in hexagonal space group $P6_3mc$ (No. 186) with $a = 3.75726(3)$ Å, $c = 11.4013(1)$ Å, and $Z = 2$. The noncentrosymmetric structure, which has few analogues, is composed of isotypic puckered hexagonal ZnS and CaO layers arranged so that ZnS₃O tetrahedra are all aligned parallel, resulting in a polar structure. The compound shows type 1 non-phase-matchable second harmonic generation, determined using 1064 nm radiation, with an efficiency approximately 100 times that of α -SiO₂ and a piezoelectric coefficient of 38 pm V⁻¹. Although polar, CaZnOS is not ferroelectric and the pyroelectric coefficient is very small, approximately 0.0 $\mu\text{C m}^{-2} \text{K}^{-1}$ between room temperature and 100 °C.

Introduction

Mixed-anion compounds such as oxychalcogenides and oxypnictides which contain both oxide anions and the anions of a heavier chalcogen (S–Te) or pnictogen (P–Sb) form a relatively rare class of compound which is receiving increasing attention. The different sizes and chemical requirements of the anions guarantee crystallographic ordering of oxide, and the larger anions and layered compounds often result. The layered oxysulfides LaCuOS¹ composed of alternating fluorite-type layers LaO and antiferrotype layers CuS have been investigated as possible transparent p-type semiconductors because the band gap in this compound lies at the edge of the visible region and the Cu-3d/S-3p antibonding crystal orbitals at the top of the valence band can readily accommodate holes generated, for example, by the substitution of La³⁺ ions by Sr²⁺ ions.² The superconducting properties of

LaFeOP with a similar structure have recently been described.³ Complex layered oxychalcogenides and oxypnictides also offer scope for the realization of new and unusual properties complementary to those found in oxides and chalcogenides as a result of control of the electronic communication between the oxide and chalcogenide layers.⁴ In this paper we describe the synthesis, the noncentrosymmetric crystal structure, and the resulting physical properties of the layered wide band gap semiconductor CaZnOS, which has been reported previously⁵ but not thoroughly characterized.

Experimental Section

Synthesis. CaZnOS was prepared on the 5 g scale by the reaction between equimolar quantities of CaO obtained from the thermal decomposition of CaCO₃ (ALFA 99.99%) and ZnS obtained by

* To whom correspondence should be addressed. E-mail: simon.clarke@chem.ox.ac.uk. Fax: +44 1865 272690. Tel: +44 1865 272600.

(1) Palazzi, M. C. *R. Acad. Sci.* **1981**, 292, 789–791.

(2) Takano, Y.; Yahagi, K.; Sekizawa, K. *Physica B* **1995**, 206–207, 764.

(3) Kamihara, Y.; Hiramatsu, H.; Hirano, M.; Kawamura, R.; Yanagi, H.; Kamiya, T.; Hosono, H. *J. Am. Chem. Soc.* **2006**, 128, 10012.

(4) Gál, Z. A.; Rutt, O. J.; Smura, C. F.; Overton, T. P.; Barrier, N.; Clarke, S. J.; Hadermann, J. *J. Am. Chem. Soc.* **2006**, 128, 8530.

(5) Petrova, S. A.; Marevich, V. P.; Zakharov, R. G.; Selivanov, E. N.; Chumarev, V. M.; Udoveva, L. Yu. *Dokl. Akad. Nauk* **2003**, 393, 52.

the reaction of zinc metal powder (Aldrich, 99.995%) and sulfur (ALFA, 99.9995%). A stoichiometric mixture was ground, pelletized, and placed in an alumina crucible, which was in turn placed in a silica tube which had been baked overnight under vacuum to remove surface moisture. The tube was sealed under vacuum and fired at 1000 °C for 4 days. The powder X-ray diffraction (PXRD) pattern of the white powder matched the simulated pattern obtained from the results in ref 5. CaO and Zn powder were handled in an argon-filled drybox, but CaZnOS was found not to be air sensitive.

Diffraction Studies. PXRD to assess phase purity was performed on a Panalytical X-pert pro diffractometer using Cu K α_1 radiation. Powder neutron diffraction (PND) data were collected at room temperature using the diffractometer POLARIS at the ISIS Facility, Rutherford Appleton Laboratory, U.K. Diffraction patterns were measured by the time-of-flight method in the d -spacing range of $0.5 < d < 8 \text{ \AA}$ using detector banks at scattering angles 2θ of 35°, 90°, and 145° for a total integrated proton current at the production target of 287 $\mu\text{A/h}$ for 2 g of CaZnOS contained in a vanadium cylinder. PND data were analyzed using the Rietveld profile refinement suite GSAS.⁶

Diffuse Reflectance Spectroscopy Measurements. Measurement was carried out at room temperature using a Varian Cary 500 UV–vis–NIR spectrophotometer equipped with a double-beam photomultiplier tube and a lead sulfide detector. Reflectance measurement of the sample was made relative to polytetrafluoroethylene: the reference material was used to establish a baseline, and the absolute reflectivity of a sample was then calculated from that of the reference. Data were collected in the wavelength range of 260–3000 nm. The Kubelka–Munk function⁷ was used to convert diffuse reflectance data to absorbance spectra.

Second Harmonic Generation (SHG). Powder SHG measurements on polycrystalline CaZnOS were performed on a modified Kurtz-NLO system⁸ using 1064 nm radiation. A Continuum Minilite II laser operating at 15 Hz was used to irradiate the sample.^{9,10} No index-matching fluid was used in any of the experiments. Because the SHG efficiency has been shown to depend strongly on particle size, polycrystalline samples were ground and sieved into distinct particle size ranges. To make relevant comparisons with known SHG materials, crystalline SiO₂ and LiNbO₃ were also ground and sieved into the same particle size ranges. Powders with particle sizes of 45–63 μm were used for comparing SHG intensities. Sieved powder samples of the specified particle size were placed in capillary tubes. The second harmonic generated light, of 532 nm wavelength, was collected in reflection and detected by a photomultiplier tube (Oriel Instruments).

Polarization Measurements. For all measurements, polycrystalline CaZnOS was pressed into 13 mm diameter and approximately 3 mm thick pellets and sintered in an evacuated silica ampule at 1000 °C (i.e., similar conditions to those used initially for synthesis). Electrodes were attached via a conducting silver paste applied to both circular faces of the pellet. Converse piezoelectric measurements were performed using a Radiant Technologies RT66A piezoelectric test system with a TREK (model 609E-6) high-voltage amplifier, Precision materials analyzer, Precision high-voltage interface, and MTI 2000 Fotonics sensor. A maximum voltage of 700 V was applied to the samples for piezoelectric

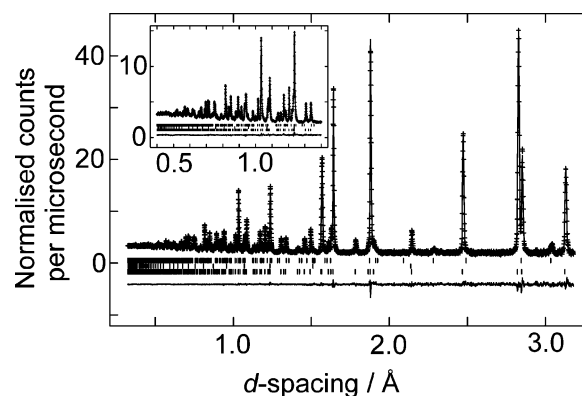


Figure 1. The results of Rietveld refinement of the structure of CaZnOS against POLARIS data. The diffractogram collected by the highest resolution 145° detector bank is shown. The data (points), fit (line), and difference plots (lower line) are shown. The reflection positions for the phases used in the refinement are shown. From bottom: CaZnOS, vanadium sample container, and a CaCO₃ impurity (1% by mass of the powder sample).

Table 1. Results of Refinement of the Structure of CaZnOS against PND Data

| | |
|---------------------------------------|--------------|
| formula | CaZnOS |
| radiation | neutron TOF |
| instrument | POLARIS |
| physical form | white powder |
| T/K | 298 |
| cryst syst | hexagonal |
| space group | $P6_3mc$ |
| fw | 153.5 |
| $a/\text{\AA}$ | 3.75726(3) |
| $c/\text{\AA}$ | 11.4013(1) |
| $V/\text{\AA}^3$ | 139.388(2) |
| Z | 2 |
| $\rho_{\text{calc}}/\text{Mg m}^{-3}$ | 3.658 |
| no. of variables | 64 |
| χ^2 | 0.852 |
| wR_p | 0.0209 |
| R_{F2} | 0.0838 |

measurements. The polarization, P , was measured on a Radiant Technologies RT66A ferroelectric test system with a TREK high-voltage amplifier between room temperature and 100 °C in a Delta 9023 environmental test chamber. The unclamped pyroelectric coefficient, p , defined as dP/dT , the change in the polarization with respect to the change in temperature, was determined by measuring the polarization as a function of temperature. The polarization was measured statically from room temperature to 100 °C in 5 °C increments, with an electric field of 4 kV cm⁻¹. The temperature was allowed to stabilize before the polarization was measured.

Results and Discussion

Crystal Structure. According to the results of laboratory PXRD studies, bulk CaZnOS was produced phase pure for the first time. Refinement of the structure against PND data confirmed the model reported from an earlier single-crystal X-ray diffraction study.⁵ However, in this earlier study the fractional occupancies of all the crystallographic atoms had been permitted to refine freely, resulting in some unphysical occupancies exceeding 1 and violating the expected charge balance. There was no indication in our refinement that any of the site occupancy factors deviated from unity; therefore, these values were fixed at this value and not refined in the final cycles. The PND experiment detected a small CaCO₃

(6) Larson, A.; von Dreele, R. B. *The General Structure Analysis System*; Los Alamos National Laboratory: Los Alamos, NM, 1985.

(7) Kubelka, P.; Munk, F. *Z. Tech. Phys.* **1931**, *12*, 593.

(8) Kurtz, S. K.; Perry, T. T. *J. Appl. Phys.* **1968**, *39*, 3798.

(9) Porter, Y.; Ok, K. M.; Bhuvanesh, N. S. P.; Halasyamani, P. S. *Chem. Mater.* **2001**, *13*, 1910.

(10) Ok, K. M.; Bhuvanesh, N. S. P.; Halasyamani, P. S. *J. Solid State Chem.* **2001**, *161*, 57.

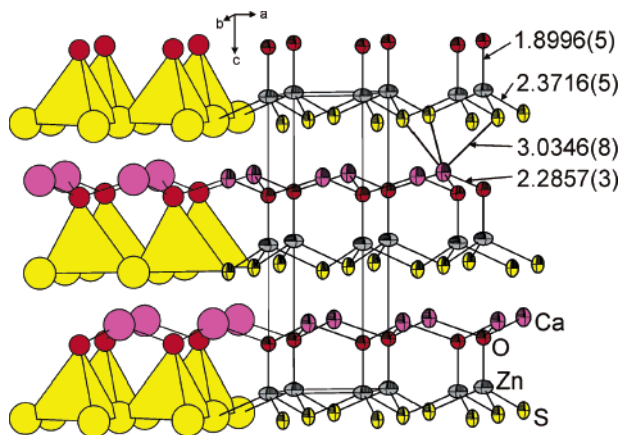


Figure 2. The crystal structure of CaZnOS. Displacement ellipsoids derived from the refinement against POLARIS data are shown at the 99% level, and selected bond lengths are given in angstroms. The left-hand part of the diagram shows ZnS_3O tetrahedra. Color Key: Ca, purple; Zn, gray; O, red; S, yellow.

Table 2. Refined Atomic Positions for CaZnOS from PND Data Collected on POLARIS

| atom | site | <i>x</i> | <i>y</i> | <i>z</i> | $U(\text{eq})^a/\text{\AA}^2 \times 100$ |
|------|------------|----------|----------|----------------|--|
| Zn | 2 <i>a</i> | 0 | 0 | 0 ^b | 0.96(2) |
| Ca | 2 <i>b</i> | 1/3 | 2/3 | 0.27021(8) | 0.82(2) |
| S | 2 <i>b</i> | 2/3 | 1/3 | 0.0841(1) | 0.65(3) |
| O | 2 <i>a</i> | 0 | 0 | 0.33338(4) | 0.67(2) |

^a $U(\text{eq})$ is defined as one-third of the orthogonalized U_{ij} tensor. ^b Not refined (i.e., Zn deemed to lie at the origin).

impurity¹¹ constituting 1% of the mass of the sample which was not observed in the laboratory PXRD measurement; this presumably derives from reaction of air with excess CaO in the as-prepared sample. No corresponding crystalline ZnS impurity was detected, so we cannot rule out that the compound is intrinsically slightly CaO deficient (1.7 mol %), but this level of deficiency is too small to be reliably determined from these data by refinement of site occupancy factors. The refinement results are shown in Figure 1 and Table 1. The refinement converged with a goodness of fit (χ^2) slightly lower than 1 (0.852), suggesting that the data had been slightly “undercollected”.

The structure is noncentrosymmetric, and the compound crystallizes in the polar space group $P6_3mc$. The structure contains two puckered hexagonal layers of similar topology of compositions CaO and ZnS. These are arranged such that Zn is tetrahedrally coordinated by three S atoms, which form part of a ZnS puckered layer, and an O atom in a neighboring CaO layer. The resulting coordination for Ca is 6-fold ($3 \times \text{O}$ and $3 \times \text{S}$). An alternative description is of layers of ZnS_3O tetrahedra all aligned with their Zn–O bond vectors parallel and directed parallel to the *c*-axis and linked at all their S-containing vertices, yielding layers ${}^{2-}_\infty[\text{ZnS}_{3/3}\text{O}]^{2-}$. Ca^{2+} cations occupy distorted octahedral interstices between these layers. The structure is shown in Figure 2, refined atomic positions are given in Table 2, and selected bond lengths and angles are given in Table 3. The Zn–O distance of 1.8996(5) Å is 4% shorter than the mean value of 1.977

(11) Pilati, T.; Demartin, F.; Gramaccioli, C. M. *Acta Crystallogr., Sect. B* **1998**, *54*, 515.

Table 3. Selected Interatomic Distances and Angles for CaZnOS

| bond | length/Å | bond angle | angle/deg |
|----------|-----------|-------------------------|-----------|
| Zn–O | 1.8996(5) | O–Zn–S [3] ^a | 113.84(3) |
| Zn–S [3] | 2.3716(5) | S–Zn–S [3] | 104.77(3) |
| Ca–O [3] | 2.2857(3) | | |
| Ca–S [3] | 3.0346(8) | | |

^a Numbers in square brackets indicate the number of symmetry equivalent bonds or angles of a particular type.

Å in wurtzite-type ZnO,¹² and the Zn–S distance of 2.3716(5) Å is consequently somewhat longer (~ 1 –1.5%) than in ZnS (mean Zn–S bond lengths of 2.335 Å in wurtzite and 2.346 Å in sphalerite).¹³ The bond distances determined by PND for CaZnOS are within 1% of the values reported from the previous single-crystal X-ray study.⁵ Bond valence calculations¹⁴ produced entirely reasonable values for the following bond valence sums: Zn, 1.99; Ca, 1.89; O, 1.86; and S, 2.02. A search of the Inorganic Crystal Structure Database showed that the closest structural analogue is CdCl(OH)¹⁵ in which formal replacement of the H atom by Zn and of the Cl atom by S yields the CaZnOS structure.

Another common structure type exhibited by oxysulfides and oxyphosphides of alkaline earths and lanthanides is that of LaCuOS¹ in which a highly chalcophilic element such as copper has only sulfide in its first coordination sphere, and the oxide ion is coordinated solely by the highly electropositive lanthanide ion. In the case of CaZnOS, zinc presumably competes effectively against calcium for the oxide ion, resulting in the ZnS_3O coordination. We have recently described the structure of BaZnOS,¹⁶ which contains an unusual network of vertex-linked ZnS_2O_2 tetrahedra in which the larger Ba^{2+} ions are accommodated in eight-coordinate sites. BaZnOS has two Zn–O distances of 1.9795(3) Å and two Zn–S distances of 2.3350(6) Å which, in contrast to the case of CaZnOS, are very similar to the distances in the binary compounds. It has not proved possible to synthesize an analogue SrZnOS: reactions between SrS and ZnO or between SrO and ZnS at temperatures between 800 and 1050 °C resulted in PXRD patterns which were fully accounted for by a mixture of SrS and ZnO. Reactions intended to produce oxyselenide analogues have been similarly unsuccessful.

Diffuse Reflectance Spectroscopy Measurements. Measurement of the absorption spectrum of CaZnOS powder using diffuse reflectance spectroscopy (Figure S1 in the Supporting Information) revealed a dominant absorption that is assigned to a room-temperature direct band gap of 3.7(1)

(12) Sawada, H.; Wang, R.; Sleight, A. W. *J. Solid State Chem.* **1996**, *122*, 148.

(13) Xu, Y.-N.; Ching, W. Y. *Phys. Rev. B* **1993**, *48*, 4335. Rabadanov, M. Kh.; Loshmanov, A. A.; Shaldin, Yu. V. *Kristallografiya* **1997**, *42*, 649.

(14) Rodriguez-Carvajal, J. Program Bond_Str, within WinPLOTR, a Windows tool for powder diffraction patterns analysis; Roisnel, T.; Rodriguez-Carvajal, J.; Materials Science Forum, In *EPDIC 7, Proceedings of the Seventh European Powder Diffraction Conference*, May 20–23, 2000, Barcelona, Spain; Delhez, R., Mittenmeijer, E. J., Eds.; Trans Tech Publications: Enfield, NH, 2001; pp 118–123.

(15) Kister, S.; Keller, H.-L.; Kockelmann, W. *Physica B* **2000**, *276*–278, 262–263.

(16) Broadley, S.; Gál, Z. A.; Corà, F.; Smura, C. F.; Clarke, S. J. *Inorg. Chem.* **2005**, *44*, 9092.

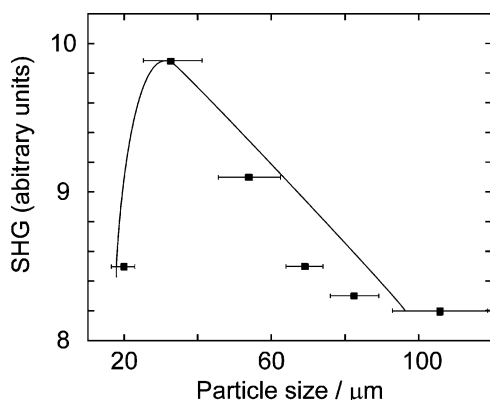


Figure 3. Second harmonic generation (SHG) efficiency of CaZnOS as a function of particle size. The line is a guide to the eye.

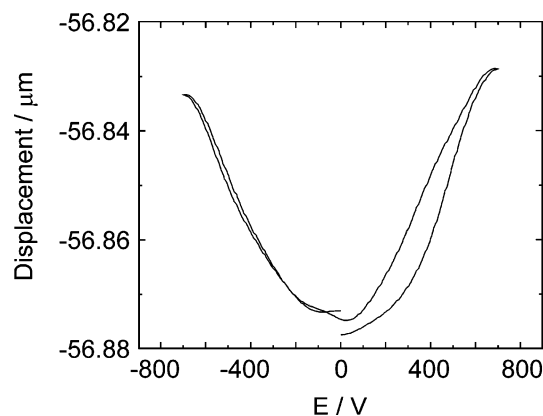


Figure 4. Piezoelectric response of CaZnOS.

eV, consistent with the white color of the compound. This value is slightly larger than the room-temperature value of 3.3 eV for wurtzite-type ZnO¹⁷ and comparable to the values of 3.67 eV obtained for sphalerite ZnS¹⁸ and 3.9(3) eV estimated for BaZnOS.¹⁶

Second Harmonic Generation and Piezoelectric Measurements. The noncentrosymmetric nature of CaZnOS suggested the material would have SHG capabilities. Powder SHG measurements performed on ground CaZnOS revealed a SHG efficiency approximately 100 times that of α -SiO₂. In addition, particle size vs SHG measurements were performed on sieved CaZnOS, to determine the type 1 phase-matching capabilities of the material. The measurements revealed that CaZnOS is not type 1 phase-matchable (see Figure 3). The efficiency and phase-matching behaviors are comparable to those of another recently reported acentric oxysulfide α -Na₃PO₃S,¹⁹ which exhibits a SHG efficiency 200 times that of α -SiO₂, and is also non-phase-matchable. In addition to measuring the SHG, we also performed piezoelectric measurements. The converse piezoelectric response for CaZnOS is shown in Figure 4. A piezoelectric coefficient, d_{33} , of 38 pm V⁻¹ was determined. This value is larger than those observed in α -SiO₂ (2.3 pm V⁻¹), wurtzite ZnO (10.6 pm V⁻¹), and CdS (10.3 pm V⁻¹) and is similar

to that of KIO₃ (39 pm V⁻¹).²⁰ The structural origin of the SHG response and the piezoelectric behavior can be attributed to the arrangement of the acentric ZnS₃O tetrahedra. These tetrahedra all point in the same [0,0,-1] direction in the structure, rendering the entire material noncentrosymmetric.

Ferroelectric and Pyroelectric Measurements. CaZnOS is not only acentric but also polar; i.e., it exhibits a dipole moment, crystallizing in the polar crystal class *6mm*. This crystal class has the correct symmetry for ferroelectric and pyroelectric behavior. Ferroelectric measurements were performed using electric fields of up to 4 kV cm⁻¹. These measurements, however, revealed no hysteresis (see Figure S2 in the Supporting Information). This is consistent with the fact that ferroelectric behavior would require the direction of the dipole moment of the ZnS₃O tetrahedron (presumably directed along the Zn–O bond) to switch under the influence of the applied electric field, and this is precluded by the crystal structure. Although the material is not ferroelectric, pyroelectric behavior is possible. We measured the change in polarization, P , as a function of temperature, $dP/dT = p$, between room temperature and 100 °C, to determine the pyroelectric coefficient, p . Our measurements revealed that between room temperature and 100 °C, $p \sim 0.0 \mu\text{C m}^{-2} \text{K}^{-1}$, a value smaller in magnitude than the values for other nonferroelectric pyroelectrics such as wurtzite ZnO, $p = -9.4 \mu\text{C m}^{-2} \text{K}^{-1}$, and CdS, $p = -4.0 \mu\text{C m}^{-2} \text{K}^{-1}$.²¹

Conclusion

CaZnOS has been prepared in bulk form for the first time, and the unusual noncentrosymmetric crystal structure has been characterized in detail using neutron powder diffraction measurements. The compound exhibits non-phase-matchable SHG with an efficiency around 100 times that of quartz and has a piezoelectric coefficient 16 times that of quartz. The compound is polar, but the crystal structure precludes ferroelectric behavior. The magnitude of the pyroelectric coefficient is very small, $\sim 0.0 \mu\text{C m}^{-2} \text{K}^{-1}$, between room temperature and 100 °C.

Acknowledgment. We thank Dr. R. I. Smith, ISIS facility, for assistance with the neutron diffraction investigations and the EPSRC for access to the ISIS facility and the Chemical Database Service at Daresbury and for the award of a studentship to C.F.S. P.S.H. thanks the Robert A. Welch Foundation for support, the NSF-Career Program through DMR-0092054, and the NSF-Chemical Bonding Center.

Supporting Information Available: For CaZnOS, optical absorbance spectrum and graphs of the room-temperature electrical polarization and function of electrical polarization vs temperature. This material is available free of charge via the Internet at <http://pubs.acs.org>.

IC062120Z

(17) Mang, A.; Reimann, K.; Rübenacke, S. *Solid State Commun.* **1995**, *94*, 251.

(18) Ves, S.; Schwarz, U.; Christensen, N. E.; Syassen, K.; Cardona, M. *Phys. Rev. B* **1990**, *42*, 9113.

(19) Takas, N. J.; Aitken, J. A. *Inorg. Chem.* **2006**, *45*, 2779.

(20) Xu, Y. *Ferroelectric Materials and Their Applications*; Elsevier Science Publishers: Amsterdam, 1991.

(21) Lang, S. B. *Phys. Today*, Aug 2005, p 31.